Journal of Engineering Physics and Thermophysics, Vol. 73, No. 1, 2000

THEORETICAL PRINCIPLES OF DESIGN OF MULTILAYER SWELLING HEAT PROTECTION WITH ASSIGNED PROPERTIES

G. N. Isakov

UDC 536.255

Theoretical principles of computer design of multilayer heat-protective coatings made of swelling materials, thermophysical and kinetic characteristics of which are found from the solution of a complex of inverse problems of heat and mass transfer and ignition, are considered. Various classes of swelling materials (including highly porous ones) and their mathematical models of thermodestruction, swelling, and breakdown are analyzed.

It is determined in [1, 2] that multipurpose multilayer swelling materials, produced from the wastes of various industries, possess the best heat-insulating properties.

When designing and using swelling materials in the systems of heat protection of space-rocket facilities one must know their thermophysical and adhesive properties and multiplicity of swelling within a wide range of temperatures, pressures, and time of their effect. These properties are a part of databases for physicomathematical models of heat and mass transfer processes and allow optimization of the heat-protective properties, composition, and arrangement of layers in coatings in designing them for specific types of products with account for different laws of heat exchange with the environment (radiative-convective [1-4], oscillatory [4], and pulse).

Methodology of Complex Investigation. The strategy of a complex investigation includes experimental study of the mechanisms of breakdown of newly developed coatings, their physicochemical properties, and creation on this basis of rather plausible mathematical models, which allow optimization of the composition and spatial arrangement of layers, for producing efficient heat protection. The main elements of this approach are presented in Fig. 1.

Reaction Cell. A reaction cell [3, 5], whose schematic diagram is given in Fig. 2, was used to study physicochemical processes occurring in swelling heat-protective materials with polymer binders. In this case, the studied specimen 1 in the form of a pellet of swelling material with the initial thickness $h_{in} = 2\,0z_1 \le 6\cdot10^{-3}$ m is placed in the reaction cell, which is the hollow cylinder 2, and allows one to study the process of swelling only along the longitudinal coordinate z. Here the condition of axisymmetry relative to $0r$ is met. The material of the cylinder (quartz, stainless steel) and its dimensions were varied in order to reveal the effect of walls on the magnitude and rate of swelling. The reaction cell is heated in the longitudinal flow 3 of a gas (nitrogen) heated to a prescribed temperature. To prevent the gas from flowing into the cell cavity, both ends of the cell are closed by the plugs 4 made of annealed asbestos board. In the experiment, the temperatures at the center 0 of the specimen T_0, on the axis of the hollow cylinder T_{0z}, and at the boundary of contact of the specimen with the cylinder wall T_{surf} are measured. The measurements are made by KhA thermocouples 5-7 [4] with a junction size of $2\cdot10^{-4}$ m; the signals from the thermocouples were recorded in time on a light-beam oscillograph [3-5].

Figure 3 presents, as an example, a typical oscillogram of the temperatures T_{surf}, T_{0z}, and T_0 (curves 1-3) as functions of the time t for a specimen made of swelling material SGK–1 [3, 5]. It is seen that the cell is heated in a linear mode (i.e., q_{surf} = const) at a rate of ~25 K/sec. Starting from $t > t_{s.r}$ ($t_{s.r}$ is the start of the

Scientific-Research Institute of Applied Mathematics and Mechanics at the Tomsk State University, Tomsk, Russia. Translated from Inzhenerno-Fizicheskii Zhurnal, Vol. 73, No. 1, pp. 52-60, January–February, 2000. Original article submitted January 27, 1999.

1062-0125/2000/7301-0049$25.00

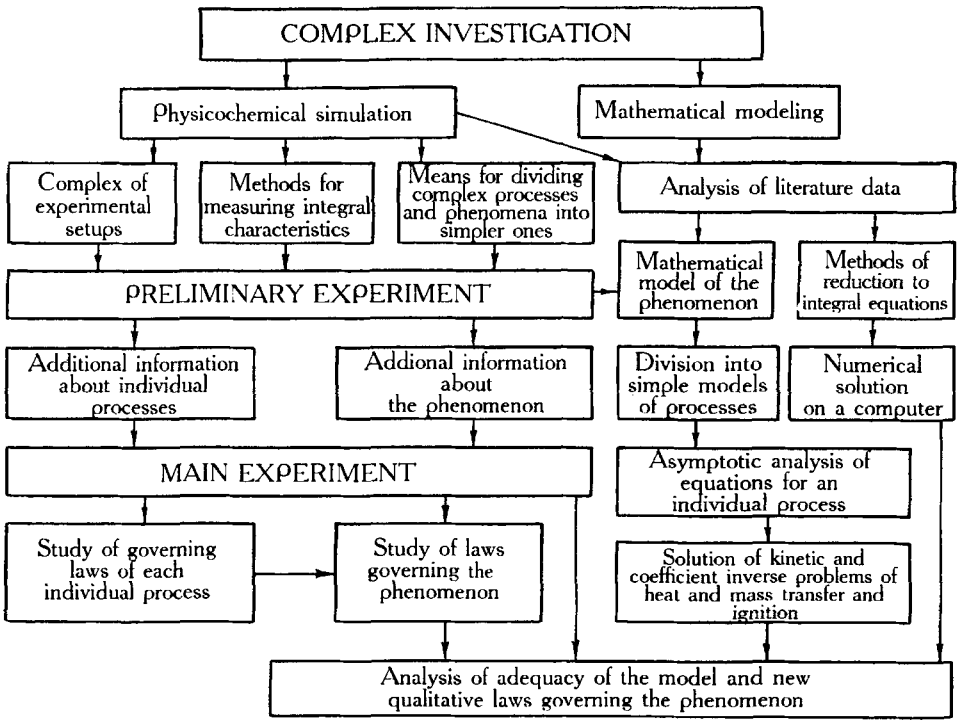

Fig. 1. Classification of the elements of complex investigation.

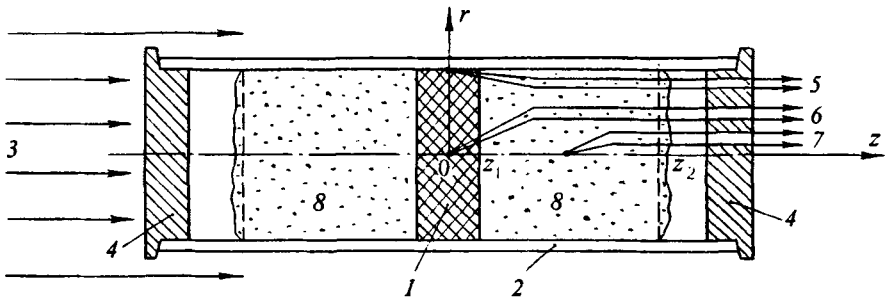

Fig. 2. Reaction cell: 1) specimen in the initial state; 2) metal hollow cylinder; 3) gas flow; 4) plugs made of asbestos board; 5-7) thermocouples; 8) specimen in the swollen state.

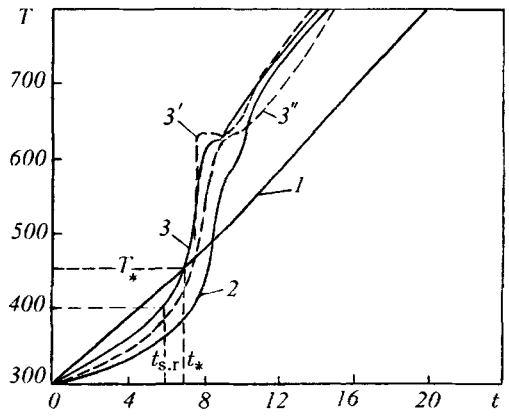

Fig. 3. Oscillogram of temperature recording: 1)$T_{surf}(t)$; 2) $T_{0z}(t)$; 3) $T_0(t)$; 3′, 3″) calculation. T, K; t, sec.

reaction of thermodestruction of the polymer binder), the temperature $T_0(t)$ increases sharply and at $t = t_*$ it becomes equal to $T_{surf}(t)$. This behavior of the curve $T_0(t)$ indicates that the thermodestruction proceeds with volumetric liberation of heat and is qualitatively similar to a solid-phase reaction with the ignition of condensed substances [4]. Adiabatic modes of these reactions are well studied and were used in [5] for determining zero approximations from kinetic parameters. Refinement was made by the solution of inverse problems [3, 6]. To determine the multiplicity of swelling and the mass loss as functions of temperature, we used the method of stabilized states [3, 5], whose modification for highly porous materials is given in [7]. Thermophysical characteristics were found from the solution of a coefficient two-dimensional inverse problem of heat conduction [3].

Mathematical Model. According to the physical interpretation of the processes observed in the experiment, we describe nonstationary heat and mass transfer in swelling material by a system of nonlinear equations of energy and chemical kinetics [3]

$$\rho c_p \frac{\partial T}{\partial t} = \frac{1}{r}\frac{\partial}{\partial r}\left(r\lambda \frac{\partial T}{\partial r}\right) + \frac{\partial}{\partial z}\left(\lambda \frac{\partial T}{\partial z}\right) - \rho c_p U \frac{\partial T}{\partial z} + \frac{\rho^0}{f(T)}(Q_1 W_1 + Q_2 W_2), \tag{1}$$

$$f(T) = 1 + \Delta h/h^0;$$

$$\frac{\partial (m/m^0)}{\partial t} + U\frac{\partial (m/m^0)}{\partial z} = W_1 + W_2;\ 0 \le t \le t_f,\ 0 \le r \le r_{surf},\ 0 \le z \le z_2(t), \tag{2}$$

with initial and boundary conditions

$$T(r, z, 0) = T^0,\ (m/m^0)(r, z, 0) = 1; \tag{3}$$

$$T(r_{surf}, z, t) = T_{surf}(z, t); \tag{4}$$

$$\frac{\partial T(0, z, t)}{\partial r} = \frac{\partial T(r, 0, t)}{\partial z} = 0; \tag{5}$$

$$\lambda(T(r, z_2, t))\frac{\partial T(r, z_2, t)}{\partial z} = \alpha_z (T_{ext.z} - T(r, z_2, t)). \tag{6}$$

Here, the rate of the reaction of thermodestruction W_1 is calculated by the formula

$$W_1 = k_{01}[(m/m^0) - (m_{f1}/m^0)]\exp(-E_1/RT). \tag{7}$$

The rate of heterogeneous reaction W_2 is found as

$$W_2 = k_{02}[(m/m^0) - (m_{f2}/m^0)]\exp(-E_2/RT). \tag{8}$$

The presence of a developed porous structure in the swollen layer 8 in Fig. 2 is a peculiar feature of the reactions. The element with the specific surface S/V should be distinguished as the characteristic dimension of the developed porous structure.

The third and fourth terms on the r.h.s. of Eq. (1) characterize the heat transfer due to the swelling and chemical reactions, respectively.

To facilitate integration of the system of equations (1)-(6) along the z axis, we pass over to new Lagrange variables [5, 6]

$$t = \tau, \quad z = \int_0^{\xi} f d\tau . \tag{9}$$

Then, the derivatives $\partial/\partial t$ and $\partial/\partial z$ and the rate of swelling U will be determined by the formulas

$$\frac{\partial}{\partial t} = \frac{\partial}{\partial \tau} - f^{-1} U \frac{\partial}{\partial \xi}, \quad \frac{\partial}{\partial z} = f^{-1} U \frac{\partial}{\partial \xi}, \quad U = \int_0^{\xi} \left(\frac{\partial f}{\partial \tau} \right) d\xi . \tag{10}$$

A variable region of integration $\{0 \le t \le t_f, 0 \le r \le r_{surf}, 0 \le z \le z_2(t)\}$ will become a constant region $\{0 \le \tau \le \tau_f, 0 \le r \le r_{surf}, 0 \le \xi \le h^0/2\}$. In the new variables ξ and τ, the system of equations (1)-(6), with account for (9)-(10), will take the form

$$\rho c_p \frac{\partial T}{\partial \tau} = \frac{1}{r} \frac{\partial}{\partial r} \left(r \lambda \frac{\partial T}{\partial r} \right) + \frac{1}{f} \frac{\partial}{\partial \xi} \left(\frac{\lambda}{f} \frac{\partial T}{\partial \xi} \right) + \frac{\rho^0}{f} (Q_1 W_1 + Q_2 W_2) ; \tag{11}$$

$$\frac{\partial (m/m^0)}{\partial \tau} = W_1 + W_2, \quad 0 \le \tau \le \tau_f, \quad 0 \le r \le r_{surf}, \quad 0 \le \xi \le h^0/2 ; \tag{12}$$

$$T(r, \xi, 0) = T^0, \quad (m/m^0)(r, \xi, 0) = 1 ; \tag{13}$$

$$T(r_{surf}, \xi, \tau) = T_{surf}(\xi, \tau) ; \tag{14}$$

$$(\lambda/f)(T(r, h^0/2, \tau)) \frac{\partial T(r, h^0/2, \tau)}{\partial \xi} = \alpha_z (T_{ext.fz} - T(r, h^0/2, \tau)) . \tag{15}$$

The two-dimensional boundary-value problem (11)-(15) was solved by the method of splitting [3, 6]. On each time half-step the obtained one-dimensional equations were solved by an iteration-interpolation method [3, 6] with iterations with respect to coefficients.

Methods for Solving Inverse Problems. One of the main stages of complex investigation of a mathematical model (see Fig. 1) is the solution of kinetic and coefficient problems of heat and mass transfer and ignition [3-7]. As an example, we consider the procedure for determining the kinetic parameters of reactions (7) and (8) and the coefficient of thermal conductivity for swelling material SGK-1 [3, 5].

The macrokinetic constants E_i, k_{0i}, and Q_i (i = 1, 2) of the reactions were found from the condition of minimum of the functional

$$J(E_1, k_{01}, Q_1, E_2, k_{02}, Q_2) = \int_0^{\tau_f} (T_0^{exp}(\tau) - T_0^{calc}(\tau))^2 dt . \tag{16}$$

Functional (16) is a root-mean-square deviation of the experimental $T_0^{exp}(t)$ and calculated $T_0^{calc}(t)$ values of the temperatures at the center of the specimen. The calculated values of the temperatures were found from the solution of the two-dimensional boundary-value problem (11)-(15). Functional (16) was minimized by the method of conjugate gradients [3, 8]. The iterative process of looking for the macrokinetic constants terminated when the condition

$$J(E_1, k_{01}, Q_1, E_2, k_{02}, Q_2) \le \delta^2 . \tag{17}$$

was met. Here $\delta^2 = \delta^2_{exp} + \delta^2_{calc}$ in the integral error of determination of the experimental (δ^2_{exp}) and calculated (δ^2_{calc}) temperatures. As a rule, $\delta^2_{calc} << \delta^2_{exp}$ [3]. The quantity δ^2_{exp} was evaluated by the formula $\delta^2_{exp} = \int_0^{\tau_f} \sigma^2(\tau)dt$, where $\sigma^2(\tau)$ is the variance of the function $T_0^{exp}(\tau)$ [4]. In practice, the parameters δ^2_{exp} and δ^2_{calc} were found from the errors of determination of the experimental (3%) [4] and calculated (0.1%) [3, 6] temperatures. In the method used, the number of iterations, consistent with condition (17), was the parameter of regularization.

As a result of the solution of the two-dimensional inverse kinetic problem we obtained the following values of macrokinetic constants for the reactions studied:

$$E_1 = (74\pm10)\ \text{kJ/mole},\ Q_1 = (1.2\pm0.2)\cdot10^6\ \text{J/kg},\ k_{01} = 1.3\cdot10^{8\pm1}\ \text{sec}^{-1};$$

$$E_2 = (43.5\pm5)\ \text{kJ/mole},\ Q_2 = (3.5\pm0.5)\cdot10^7\ \text{J/kg},\ k_{02} = 5\cdot10^{2\pm0.5}\ \text{sec}^{-1}.$$

Dashed curves *3′* and *3″* in Fig. 3 show the calculated dependences of the temperature at the center of the specimen obtained by solving a two-dimensional direct problem with the macrokinetic constants from the present work (*3′*) and from [8] (*3″*). In [8], the macrokinetic constants were found by solving a one-dimensional inverse problem. The better agreement between curves *3* and *3′* is explained by the fact that in solving a two-dimensional inverse kinetic problem account is taken of the heat overflow along the $0z$ axis which takes place in the physical experiment.

Influence of the Pressure and Composition of the External Medium. For studying the effect of the parameters of the external medium on the processes of swelling and heat and mass transfer, the reaction cell presented in Fig. 2 was placed in a bomb of constant pressure [9]. In this case, the experiment is automated by pneumoautomatics. The capabilities of the experiment are as follows: pressure range $(1-10)\cdot10^{-5}$ Pa; composition of medium: nitrogen, air, and argon; heat fluxes from $5\cdot10^3$–$5\cdot10^5$ W/m^2.

Multilayer Coatings. Provision of the refractoriness of structures due to the use of fireproof coatings is an integral part of the system of measures on fire safety of buildings, constructions, and objects of space-rocket engineering.

For the mass thermal tests of multilayer heat-protective coatings under the conditions of the thermal effect of crown forest fire, use was made of a proving-ground simulator which is a burning stockpile of commercial timber [10]. The scheme of a multilayer structure where a three-layer fireproof material was deposited onto a metal substrate and the rear side was insulated is given in Fig. 4. The experimentally measured temperature of the substrate was compared to the calculated temperature determined numerically by solution of the problem [2, 6] based on the known conditions on a thermally stressed surface $y = y_5(t)$.

Figure 5 presents the experimental dependence of the total heat flux density $q_{surf\Sigma}$ on the time t and the calculated temperatures on heated (T_{surf}) and rear (T_2) surfaces of fireproof materials. It is known that a capillary-porous structure greatly affects the processes of heat and mass transfer in heated layers of heat-protective and fireproof coatings [1-7]. In particular, at high heat fluxes, processes of swelling take place in the coatings [5-8], which increase the thickness and porosity of the heat-protective layer and decrease of the coefficient of thermal conductivity and density of the material. If moisture is accumulated in the porous structure of a coating, which is typical of exploitation of coatings under natural conditions, it exerts a negative effect on their adhesive properties, but improves the heat-protective properties due to the expenditure of energy on phase transition [2], redistribution of temperature fields, and decrease in the rate of heat transfer of the coatings in high-temperature gas flow.

Mathematically, the process of heat and mass transfer in the considered five-layer plate is described by the system of equations [6]

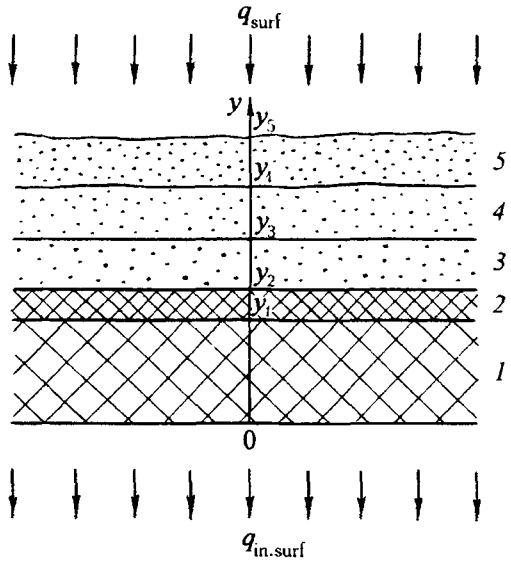

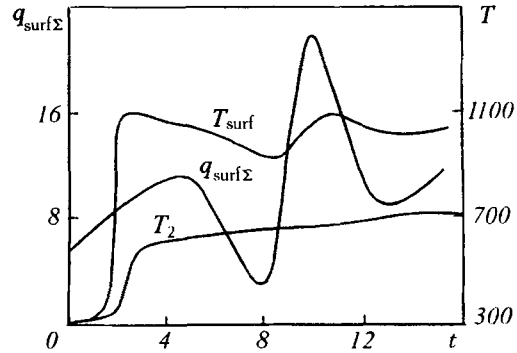

Fig. 4. Scheme of a thermal experiment: 1) insulator; 2) metal substrate; 3-5) fireproof material.

Fig. 5. Heat flux from the actual fire $q_{surf\Sigma}$ and calculated temperatures T_{surf} and T_2 vs. time t. $q_{surf\Sigma}$, kW/m^2; t, min.

$$(\rho c_p)_i \frac{\partial T_i}{\partial t} = \frac{\partial}{\partial y}\left(\lambda_i \frac{\partial T_i}{\partial y}\right), \quad i = \overline{1,3}; \tag{18}$$

$$(\rho c_p)_i \frac{\partial T_i}{\partial t} = \frac{\partial}{\partial y}\left(\lambda_i \frac{\partial T_i}{\partial y}\right) - [(\rho c_p)_i U_i + \varphi_{gi} (\rho_g c_{pg})_i u_{gi}] \frac{\partial T_i}{\partial y} - Q\rho_m \varphi_{mi} W_i; \tag{19}$$

$$\frac{\partial (\rho_{gi} \varphi_{gi})}{\partial t} + \frac{\partial (\rho_{gi} \varphi_{gi} U_i)}{\partial y} + \frac{\partial (\rho_{gi} \varphi_{gi} u_{gi})}{\partial y} = \alpha_v \rho_m \varphi_{mi} W_i; \tag{20}$$

$$P_i \frac{\rho_{gi} R T_i}{M_g}; \quad u_{gi} = -\frac{k_{gi}}{\mu_{gi}} \frac{\partial P_i}{\partial y}; \tag{21}$$

$$\frac{\partial \varphi_{gi}}{\partial t} + U_i \frac{\partial \varphi_{gi}}{\partial y} = -W_i; \quad \frac{\partial \varphi_{si}}{\partial t} + U_i \frac{\partial \varphi_{si}}{\partial y} = 0; \tag{22}$$

$$\varphi_{gi} = 1 - \varphi_{si} - \varphi_{mi}; \quad W_i = \varphi_{mi} k_0 \exp\left(-\frac{L}{RT_i}\right), \quad k_{gi} = k_* \varphi_{gi}^3 (1 - \varphi_{gi})^{-2}, \quad i = 4, 5. \tag{23}$$

System (18)-(23) consists of the equations of heat conduction and energy conversion (18), (19), the continuity equations (20), the equations of state and momentum conservation in the form of Darcy's linear law (21) [3, 4, 6] for the products of moisture evaporation and thermodestruction, the equation of mass conservation for the moisture and the filler (22), and the algebraic integral (23) for the bulk fraction of the products of moisture evaporation and thermodestruction. The permeability coefficient k_{gi} is determined by the Kozeny–von Kármán formula [6]. The continuity equations (20), after substitution of density ρ_{gi} and rate of filtration u_{gi} from (21), are transformed to parabolic equations for pressure p_i.

The system of equations (18)-(23) is supplemented by the initial and boundary conditions

$$t = 0: \quad T_i = T_i^0, \quad p_i = p_i^0, \quad \varphi_{mi} = \varphi_{mi}^0, \quad \varphi_{si} = \varphi_{si}^0; \tag{24}$$

$$y = 0: \quad -\lambda_1 \frac{\partial T_1}{\partial y} = \alpha_{in.s} (T_{g.in.s} - T_{in.s}); \tag{25}$$

$$y = y_3: \quad \frac{\partial p_4}{\partial y} = 0, \quad \varphi_{m4} = \varphi_{m4}^*, \quad \varphi_{si} = \varphi_{si}^*; \tag{26}$$

$$y = y_i: \quad T_i = T_{i+1}, \quad \lambda_i \frac{\partial T_i}{\partial y} = \lambda_{i+1} \frac{\partial T_{i+1}}{\partial y}, \quad i = \overline{1,4}; \tag{27}$$

$$y = y_4: \quad p_4 = p_5, \quad \frac{p_{g4} \varphi_{g4} k_{g4}}{\mu_{g4}} \frac{\partial p_4}{\partial y} = \frac{p_{g5} \varphi_{g5} k_{g5}}{\mu_{g5}} \frac{\partial p_5}{\partial y}, \quad \varphi_{m5} = \varphi_{m5}^*; \quad \varphi_{s5} = \varphi_{s5}^*; \tag{28}$$

$$y = y_5: \quad \lambda_5 = \frac{\partial T_5}{\partial y} = \alpha_{surf} (T_{g.ext.f} - T_{surf}) + A_{eff} \sigma (T_{fl}^4 - T_{surf}^4), \quad p_5 = p_{ext.f}. \tag{29}$$

The given mathematical model (18)-(29) serves for determination of the functions T_i ($i = \overline{1,5}$), p_i, ρ_{gi}, u_{gi}, φ_{mi}, φ_{si}, and φ_{gi} (i = 4, 5).

Experimental data on the curves of swelling $f_i(T) = 1 + \Delta h_i / h_i^0$ ($\Delta h_i = h_i - h_i^0$ is the variation in the thickness of coating layers) [2, 3, 6, 8], initial mass concentrations, and thermophysical characteristics (TPCs) of components of the layers were used to close the mathematical model (18)-(29). Termophysical characteristics of layers 4 and 5 (see Fig. 4) were found in terms of true TPCs and bulk fractions of the components of these layers. The function A_{eff} was determined by the Christiansen formula [4, 6]. Blowing out of evaporation (thermodestruction) products was taken into account in calculation of the coefficient of heat transfer α_{surf}.

To facilitate a numerical solution of the problem, transition to the Lagrange variables was undertaken in the mathematical model (18)-(29) [6]. Parabolic equations for determination of temperature and pressure were solved by an iteration-interpolation method [3, 6, 8].

Design of Heat-Protective Materials. In accordance with the suggested methodology, environmentally clean fireproof evaporating coatings (FECs), developed at the Scientific-Research Institute of Applied Mathematics and Mechanics at the Tomsk State University, were designed using a computer. The following materials of the layers were used (see Fig. 4): 1, insulator (y_1 = 20 mm); 2, steel substrate $y_2 - y_1$ = 2.4 mm); 3, fireproof material FEC ($y_3 - y_2$ = 1.5 mm); 4, porous FCE ($y_4^0 - y_3$ = 1.5 mm); 5, glass fiber ($y_5^0 - y_4^0$ = 1.5 mm). The arrangement of layers 3–5 and the initial mass concentrations of moisture C_{mi}^0 in layers 4 and 5 varied. Within the temperature range of (290–650) K the multiplicities of swelling $\Delta h_i / h_i^0$ varied from 0 to 2. Thermokinetic constants for the process of volumetric evaporation of moisture are borrowed from [4] and the remaining values of the input parameters from [2-4, 6].

Figure 6 presents the dependences of the temperature of the heated surface T_{surf} (upper curves) and the substrate T_2 (lower curves) on time for various materials of layers 3–5 without (solid curves) and with (dot-dash curves) regard to the moisture in layers 4 and 5. Curves 1 correspond to the arrangement of materials in the layers: 3, glass fiber; 4, porous FEC; 5, FEC; curves 2: 3, FEC; 4, porous FEC; 5, glass fiber. The time of attaining the limit of refractoriness t_{refr} is 15.1 min for the first case and 44.8 min for the second case. Upon saturation of layers 4 and 5 with moisture of $C_{m4}^0 = C_{m5}^0 = 0.2$, the time t_{refr} increases from 17.1 to 50.7 min,

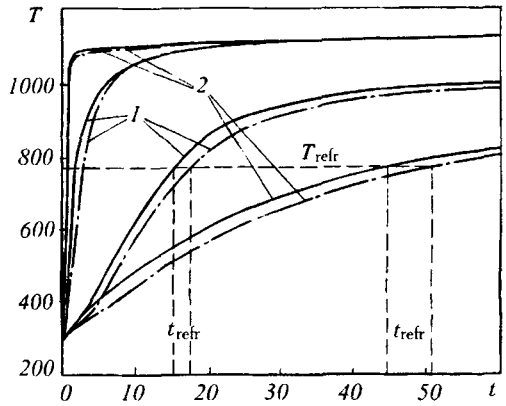

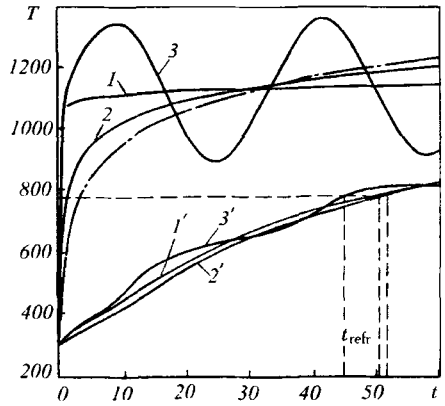

Fig. 6. Dependences $T_{surf}(t)$ and $T_2(t)$ for various layers.

Fig. 7. Dependences $T_{surf}(t)$ (curves 1-3) and $T_2(t)$ (curves 1′-3′) for the optimum composition of materials of layers.

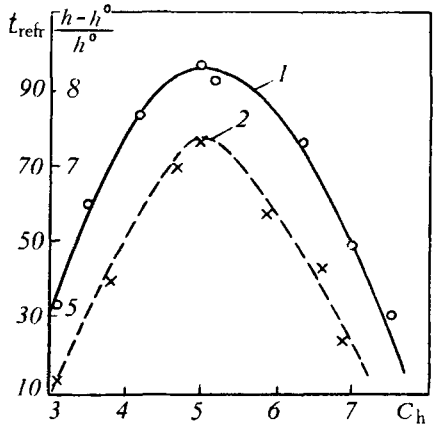

Fig. 8. Refractoriness limit t_{refr} (1) and multiplicity of swelling $(h - h^0)/h^0$ (2) vs. mass concentration of hardener C_h in an FEC coating. t_{refr}, min; C_h, %.

respectively. Thus, the highest effect of fire protection is achieved when materials with low thermal conductivity, density, and high porosity are placed closer to the heated surface.

Figure 7 presents the dependences of T_{surf} and T_2 on t which are obtained for the optimum choice of materials of the layers (3, FEC; 4, porous FEC; 5, glass fiber) at $C^0_{m4} = C^0_{m5} = 0.2$ for various laws of $T_{g.ext.f}$ variation. Here, curves *1* and *1′* are obtained for a constant temperature $T_{g.ext.f} = 1100$ K; *2* and *2′*, temperature $T_{g.ext.f}$ varies in the mode of "standard fire" [1] (dot-dash curve); *3* and *3′*, sinusoidal temperature variation $T_{g.ext.f}(t) = \overline{T_{g.ext.f}} + A \sin 2\pi\nu t$ or $T_{fl}(t) = \overline{T_{fl}} + A \sin 2\pi\nu t$ [4, 6]. Here $\overline{T_{g.ext.f}} = 1100$ K and $\overline{T_{fl}} = 1200$ K are the mean values of temperature; $A = 220$ K is the amplitude of oscillations; $\nu = 5 \cdot 10^{-4}$ sec^{-1} is the frequency of oscillations. The values of t_{refr}, viz., 1, 50.7 min; 2, 51.2 min; 3, 45.4 min correspond to these cases. An analysis of Fig. 7 shows that all the thermal tests and calculations were made under more "rigid" conditions of the heat load than in "standard fire" [1, 6]. In estimating the refractoriness limit t_{refr} of structures under the conditions of the actual fire, one should allow for low-frequency oscillations of the external flow and flame. For example, with a decrease in ν from $5 \cdot 10^{-4}$ sec^{-1} to 10^{-4} sec^{-1} the time t_{refr} decreases from 45.4 min to 35.9 min. An increase in the initial mass concentration of moisture from 0 to 0.3 increases the time t_{refr} from 44.8 to 53.0 min. Qualitatively similar results are obtained when polymer binder-based swelling materials are used in a fireproof coating [1, 3-5].

To improve the technological conditions of deposition of the produced coatings onto a metal structure and to decrease their drying time, we introduced hardeners, which, under the thermal effect, increase the porosity and gas liberation in a swollen layer. The dependences of the multiplicity of swelling and the refractoriness limit of FEC on the content of a hardener are shown in Fig. 8. The optimum content of hardeners (~4.5%) in FEC coatings, which provides a refractoriness of ~1.5 h with a coating thickness of $\sim 4 \cdot 10^{-3}$ m, was determined from these data. Coatings of this type are recommended for practical use.

CONCLUSIONS

1. A strategy for complex investigation of heat-protective properties of porous materials required for the design of a multilayer swelling heat protection is suggested.

2. A reaction cell and a two-dimensional mathematical model, which allow one to study physicochemical transformations in swelling materials and to determine macrokinetic and thermophysical characteristics by solution of inverse problems, are described.

3. A physicomathematical model of heat and mass transfer in multilayer swelling coatings, which makes it possible to transfer results of laboratory fire tests to the conditions of the actual fire by computer simulation, is presented.

4. Certain results of designing multilayer coatings using the optimum relation between the thickness and the spatial arrangement of the layers, and also by choosing components with assigned thermophysical properties in each layer, are presented.

NOTATION

t, time; T, temperature; r, y, z, coordinates; q, heat flux; ρ, density; c_p, heat capacity; λ, thermal conductivity; U, rate of swelling; m, mass; h, thickness of the pellet made of swelling material; α, coefficient of heat transfer; E_1, k_{01}, Q_1, energy of activation, preexponent, and thermal effect of the thermodestruction reaction; E_2, k_{02}, Q_2, ν_2, energy of activation, preexponent, thermal effect, and order (with respect to oxidizer) of the heterogeneous reaction; P_2, M_2, C_2, pressure, molecular mass, and concentration of oxidizer in the porous structure; S/V, specific surface; S, surface; V, volume; $z_2(t)$, moving boundary of the swollen layer; $k_{02} = \overline{k_{02}}(S/V)(P_{ext.f2}M_{ext.f2}C_{ext.f2}/RT_*)^{\nu_2}$, effective value of preexponential factor; p, pressure; C, concentration; φ, bulk fraction; u_g, rate of filtration of evaporation (thermodestruction) products; μ, dynamic viscosity; W, rate of moisture evaporation or reaction of thermodestruction; L, k_0, Q, energy of activation, preexponent, and thermal effect of the evaporation process; α_ν, reduced stoichiometric number; A_{eff}, effective function of radiation parameters of the coating and the flame; σ, Stefan–Boltzmann constant; R, universal gas constant; y_i, coordinates of boundaries of layers. Superscript: 0, initial; subscripts: f, final; g, gaseous; s, solid, stabilization at given temperature; *, characteristic; m, moisture; fl, flame; ext.f, external flow; surf, heated surface; in.surf, inner surface; refr, refractoriness; h, hardener; $i = \overline{1,5}$, numbers of layers.

REFERENCES

1. I. G. Romanenkov and F. A. Levites, *Fire Protection of Constructions* [in Russian], Moscow (1991).
2. G. N. Isakov, A. Ya. Kuzin, and A. V. Perevalov, in: *"Heat and Mass Transfer–MIF-96." Heat and Mass Transfer in Capillary-Porous Bodies: Proc. 3rd Minsk Int. Forum*, Minsk, May 20-24, 1996 [in Russian], Vol. 7, Minsk (1996), pp. 113-117.
3. G. N. Isakov and A. Ya. Kuzin, *Prikl. Mekh. Tekh. Fiz.*, **37**, No. 4, 126-134 (1996).
4. G. N. Isakov, *Modeling of Nonstationary Processes of Heat and Mass Transfer and Ignition in Reactive Media* [in Russian], Tomsk (1988).
5. G. N. Isakov and V. V. Nesmelov, *Fiz. Goreniya Vzryva*, **30**, No. 2, 57-63 (1994).
6. G. N. Isakov and A. Ya. Kuzin, *Fiz. Goreniya Vzryva*, **34**, No. 2, 82-89 (1998).

7. G. N. Isakov and A. Ya. Kuzin, in: *Heat Transfer and Thermophysical Properties of Materials, Proc. All-Union Seminar* [in Russian], Novosibirsk (1992), pp. 235-241.
8. G. N. Isakov and A. Ya. Kuzin, in: *Proc. 2nd Int. Conf. "Identification of Dynamic Systems and Inverse Problems," [in Russian], Pt. 2, St. Petersburg (1994), pp. D-5-1–D-5-10.*
9. G. N. Isakov, in: *Conjugate Problems of Mechanics and Ecology, Proc. Int. Conf.* [in Russian], Tomsk (1996), p. 113.
10. G. N. Isakov, A. Ya. Kuzin, A. I. Kosogov, et al., in: *Conjugate Problems of Physical Mechanics and Ecology, Proc. Int. Conf.* [in Russian], Tomsk (1994), p. 85-86.
11. G. N. Isakov, A. Ya. Kuzin, E. V. Lavrinenko, and A. V. Perevalov, in: *Abstr. 1st Int. Symp. "Advanced Thermal Technologies and Materials,"* Katsiveli, Crimea, September 22–26, 1997 [in Russian], Moscow (1997), p. 194.